

Article

Enhanced Built-Up and Bareness Index (EBBI) for Mapping Built-Up and Bare Land in an Urban Area

Abd. Rahman As-syakur ^{1,*}, I Wayan Sandi Adnyana ^{1,2}, I Wayan Arthana ¹ and I Wayan Nuarsa ^{1,2}

¹ Environmental Research Center (PPLH), Udayana University, PB Sudirman Street, Denpasar, Bali 80232, Indonesia; E-Mail: iwarthana60@yahoo.co.id

² Faculty of Agriculture, Udayana University, Kampus Bukit Jimbaran, Bali 80361, Indonesia; E-Mails: sandiadnyana@yahoo.com (I.W.S.A.); nuarsa@ymail.com (I.W.N.)

* Author to whom correspondence should be addressed; E-Mail: ar.assyakur@pplh.unud.ac.id; Tel.: +62-361-236-221; Fax: +62-361-236-180.

Received: 20 August 2012; in revised form: 21 September 2012 / Accepted: 24 September 2012 /

Published: 2 October 2012

Abstract: Remotely sensed imagery is a type of data that is compatible with the monitoring and mapping of changes in built-up and bare land within urban areas as the impacts of population growth and urbanisation increase. The application of currently available remote sensing indices, however, has some limitations with respect to distinguishing built-up and bare land in urban areas. In this study, a new index for transforming remote sensing data for mapping built-up and bare land areas is proposed. The Enhanced Built-Up and Bareness Index (EBBI) is able to map built-up and bare land areas using a single calculation. The EBBI is the first built-up and bare land index that applies near infrared (NIR), short wave infrared (SWIR), and thermal infrared (TIR) channels simultaneously. This new index was applied to distinguish built-up and bare land areas in Denpasar (Bali, Indonesia) and had a high accuracy level when compared to existing indices. The EBBI was more effective at discriminating built-up and bare land areas and at increasing the accuracy of the built-up density percentage than five other indices.

Keywords: Enhanced Built-Up and Bareness Index; NIR; SWIR; TIR

1. Introduction

One of the main problems in mapping urban areas is assessing the change in land usage from non-residential to residential. Land use changes usually occur because of high urbanisation and residential development rates. These conditions result in high surface runoff, changes in micro-temperature [1], transport of water pollutants [2], and reduction in water quality [3]. In some cases, development may introduce bare land within an urban area [4]. This bare land is seasonal due to the effect of land use changes or the timing of fallow periods in paddy fields after harvesting.

Mapping the built-up and bare land in urban areas is important because the existence of these types of land can be used as an indicator of urban development and environmental quality [5]. The mapping process applies different remotely sensed data and spectral values based on the land use category. Land use mapping primarily employs the multispectral classification method; however, there are other methods that also utilise the application of the remote sensing index [1]. Chen *et al.* [6] classified urban land uses using several remote sensing indices in the Pearl River Delta of China with high accuracy. Indices for mapping the built-up and bare land in urban areas, such as the Normalised Difference Built-Up Index (NDBI) [7], Index-based Built-Up Index (IBI) [1], Urban Index (UI) [8], Normalised Difference Bareness Index (NDBaI) [4], and Bare soil index (BI) [9], have been employed in various studies.

NDBI and UI are based on the high-speed mapping of built-up or bare land areas. Nevertheless, these two indices are unable to verify the distribution of built-up versus bare land areas [7,10,11]. He *et al.* [10] stated that this inability was due to the high complexity of the spectral response patterns to vegetation, bare land, and built-up areas, particularly in terms of the pixel combinations in areas with heterogenic objects.

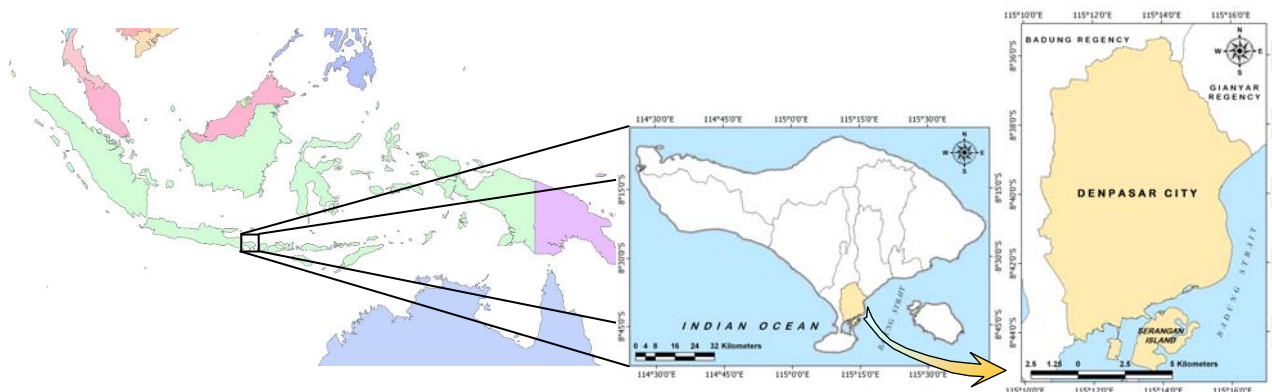
This paper introduces a new index for mapping built-up and bare land areas. This index, referred to as the Enhanced Built-Up and Bareness Index (EBBI), is able to map and distinguish built-up and bare land areas and was tested by mapping these land use categories in the city of Denpasar (Bali, Indonesia). The EBBI mapping results were compared to the results of other remote sensing indices. The relationship between the amount of built-up cover from EBBI and that from other remote sensing indices was also determined. The results of this study provide an alternate and more accurate remote sensing index for mapping built-up and bare land areas.

2. Research Location

The study was conducted in Denpasar (Bali, Indonesia), which is located at 08°35'31"–08°44'49" south latitude and 115°10'23"–115°16'27" east longitude (Figure 1) with an area of 125.95 km². Denpasar city is bordered by Badung Regency to the north and west, Gianyar Regency to the east, and the Badung Strait area to the south. A small island, Serangan Island, is located in the southern part of Denpasar. In 2010, the population of Denpasar city reached 788,589 people, with an average growth rate of 3.55% per year [12]. The slope morphology in the Denpasar area is from 0 to 8%, and the altitude ranges from 0 to 75 m above sea level. The climate of Denpasar is influenced by monsoon activity [13,14]. The monthly average temperature of Denpasar is 24–32 °C, and the average monthly rainfall is 13–358 mm. Land use within the study area includes 7 different classes: settlement, paddy

field, perennial plant, bare land, forest (mangrove), dry land, and shrub. Settlement is the dominant land use, followed by paddy field and perennial plant areas [15].

Figure 1. Research Location.



3. Method

3.1. Enhanced Built-Up and Bareness Index (EBBI)

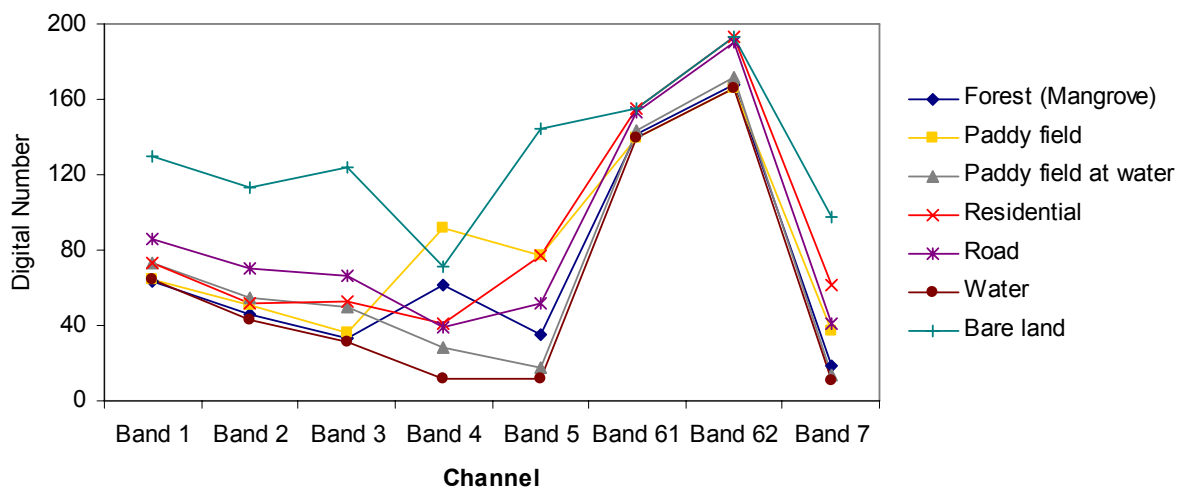
The EBBI is a remote sensing index that applies wavelengths of 0.83 μm , 1.65 μm , and 11.45 μm , (NIR, SWIR, and TIR, respectively) to Landsat ETM+ images. These wavelengths were selected based on the contrast reflection range and absorption in built-up and bare land areas. According to Herold *et al.* [16], the reflectance values of built-up areas are higher due to the longer sensor wavelengths. The NIR wavelength, which corresponds to band 4 in Landsat ETM+ and band 5 in SWIR, is associated with a high contrast level for detecting built-up and bare land areas, as shown in Figure 2. In addition, in bands 4 and 5, there is an inverse reflectance ratio with respect to detecting built-up or bare land areas compared to vegetation. Vegetation has a high reflectance in band 4, but the reflectance of built-up or bare land in band 4 is low. In contrast, in band 5, there is high reflectance when detecting built-up areas compared with vegetated areas [17]. NIR and SWIR were used for mapping built-up areas in a study conducted by Zha *et al.* [7] when developing the NDBI.

Zhao and Chen [4] utilised Landsat ETM+ band 5 (SWIR) and band 6 (TIR) to generate the NDBaI. The NDBaI is an index used to map bare land areas. The TIR can distinguish high and low levels of albedo in built-up objects [4]. According to Weng [5], the utilisation of TIR channels is very effective for mapping built-up areas based on a low albedo, which eliminates the effect of shadows and water, while a high albedo demonstrates built-up and bare land areas clearly. The TIR channel also exhibits a high level of contrast for vegetation. The temperature of a built-up area is 10–12 degrees higher than that of vegetation [18]. Therefore, the combination of NIR, MIR, and TIR (Landsat ETM+ bands 4, 5, and 6) wavelengths makes it possible to improve the mapping method for built-up and bare land areas relative to previously existing remote sensing indices.

By combining the NIR, MIR, and TIR (Landsat ETM+ bands 4, 5, and 6) wavelengths, the subtraction of band 4 from band 5 will result in positive values for built-up and barren pixels and will result in negative values for vegetation. In addition, a summation of band 5 and band 6 will result in higher values pixel for built-up and bare land than for vegetation. The difference between the subtraction of band 4 from band 5 and the summation of band 5 and band 6 will result in virtually 0

water pixels as well as negative values for vegetation and positive values for built-up and barren pixels. This outcome allows for easy distinguishing between built-up and bare land areas.

Figure 2. Spectral profiles for seven classes of land cover in Denpasar city. Values were derived from an average of 20 pixels for each class of land cover.



To achieve a higher level of contrast, an improvement in the mathematical operations was introduced into the equation used to calculate the EBBI. The EBBI applies a root function to cluster the numbers that contrast identical objects based on the different levels of reflectance values. To obtain an index value of $-1 \sim 1$, the multiplied factor is divided by ten. The EBBI is calculated from the image data using the following formula:

$$EBBI = \frac{\text{Band 5} - \text{Band 4}}{10\sqrt{\text{Band 5} + \text{Band 6}}} \quad (1)$$

3.2. Data and Analysis

3.2.1. Data

The remote sensing data used in this study were Landsat ETM+ data acquired on 21 May 2002 in Path 116 and Row 66. The spectral wavelength ranges and the spatial resolution bands of the data are presented in Table 1 [19]. The accuracy levels of the analyses performed using several remote sensing indices were compared to the distribution of built-up and bare land areas in the IKONOS imagery analysis. The IKONOS image used for comparison was acquired on 22 April 2002. The interpretation of the distribution of built-up and bare land originated from the Regional Planning and Development Board of Denpasar in 2003. The classification of the IKONOS image had an overall accuracy rate of 96.4%.

3.2.2. Analysis

The main analysis performed throughout this study was an application of the EBBI for mapping built-up and bare land areas. Another analysis was conducted in this study to determine the relationship between the EBBI and the percentage of built-up area in the Denpasar region. To determine the effectiveness of the EBBI for mapping built-up and bare land areas, the results of the

EBBI analysis were compared to the results of remote sensing analyses that used several other indices: the IBI, NDBI, UI, NDBaI and NDVI (Normalised Difference Vegetation Index) [20]. The IBI, NDBI, and UI are indices for quickly mapping built-up areas. In contrast, the NDVI is a well-known spectral index for rapidly mapping the distribution of vegetation and a variety of conditions over land surfaces. Previously, Matthias and Martin [21] applied NDVI for mapping the impervious area of an urban area of Germany. The formulas for the indices that were compared to the EBBI results are as follows:

$$IBI = \frac{2\text{Band } 5 / (\text{Band } 5 + \text{Band } 4) - [\text{Band } 4 / (\text{Band } 4 + \text{Band } 3) + \text{Band } 2 / (\text{Band } 2 + \text{Band } 5)]}{2\text{Band } 5 / (\text{Band } 5 + \text{Band } 4) + [\text{Band } 4 / (\text{Band } 4 + \text{Band } 3) + \text{Band } 2 / (\text{Band } 2 + \text{Band } 5)]} \quad (2)$$

$$NDBI = \frac{\text{Band } 5 - \text{Band } 4}{\text{Band } 5 + \text{Band } 4} \quad (3)$$

$$UI = \frac{\text{Band } 7 - \text{Band } 4}{\text{Band } 7 + \text{Band } 4} \quad (4)$$

$$NDBaI = \frac{\text{Band } 5 - \text{Band } 6}{\text{Band } 5 + \text{Band } 6} \quad (5)$$

$$NDVI = \frac{\text{Band } 4 - \text{Band } 3}{\text{Band } 4 + \text{Band } 3} \quad (6)$$

where the pixel value used in each channel is the digital number. In this study, the EBBI and NDBaI utilised band 6 of the Landsat ETM+ images; band 6 has a 60 m spatial resolution, which was rescaled to 30 m prior to transforming the data into an index.

Table 1. Spectral Bands of Landsat ETM+.

Channel	Spectral Range (μm)	Spatial Resolution (m)	Electromagnetic Region	Application
Band 1	0.45–0.52	30	Visible Blue	Coastal water mapping, differentiation of vegetation from soils
Band 2	0.53–0.61	30	Visible Green	Assessment of vegetation vigour
Band 3	0.63–0.69	30	Visible Red	Chlorophyll absorption for vegetation differentiation
Band 4	0.78–0.90	30	Near Infrared	Biomass surveys and delineation of water bodies
Band 5	1.55–1.75	30	Short Wave Infrared	Vegetation and soil moisture measurements
Band 6	10.4–12.5	60	Thermal Infrared	Land surface temperature
Band 7	2.09–2.35	30	Short Wave Infrared	Hydrothermal mapping
Band 8	0.52–0.90	15	Panchromatic	Visual interpretation

Comparison and validation of the analysis results was performed using IKONOS data. The results of the interpretation of built-up and bare land areas from the IKONOS image by the Regional Planning and Development Board of Denpasar were assumed to represent the actual distribution of built-up and bare land areas. The built-up and bare land areas were obtained from the visual interpretation of the data in vector form, which was then converted into 30 × 30 m pixels in raster form. The raster data were used to compare the results of the transformation analysis. The bare land areas in Denpasar city consist of rice fields in the fallow period after harvesting and soil areas following the reclamation of

Serangan Island. To determine the accuracy of the EBBI, this study examined bare land located in Serangan Island. The validation process was accomplished by comparing the built-up and bare land areas determined by the indices (EBBI, IBI, NDBI, UI, NDBaI and NDVI) with the results from IKONOS. Comparative results were based on the differences in the areal percentage, which were used to determine the level of accuracy.

The percentage of built-up areas was obtained from the IKONOS image analysis. The percentage of built-up area refers to the proportion of built-up area within each pixel. Fifty built-up locations were randomly selected, and polygon sampling of the data was conducted based on the number of Landsat pixels in the image (30×30 m). The percentage of built-up areas was correlated to the remote sensing index to determine the relationship between the percentage of built-up areas and the remote sensing indices. The mean bias error (MBE) and the root mean square error (RMSE) [22,23] were used to calculate the systematic and non-systematic errors of each of the transformation indices. MBE is a good measure of model bias and is simply the average of the differences in the set. The RMSE was used to find the average error value between the remote sensing indices and the percentage of built-up areas.

4. Results

The transformation of bands 4, 5, and 6 of Landsat ETM+ was examined in this study. This study investigated the mapping of built-up and bare land areas by EBBI transformation. The EBBI transformation was compared to other transformation indices. The results of the EBBI transformation were compared to the results obtained using IKONOS imagery to determine the levels of accuracy and effectiveness. In addition, the results of comparing the relationship between the EBBI and the percentages of built-up area coverage and remote sensing indices are detailed in this section.

Transforming remote sensing data into an index value required the use of a control index value as a reference index to distinguish the different types of land cover. In this case, the reference was the limit of the index value for each type of transformation index, as shown in Table 2.

Table 2. Limitation of the index value for each type of index transformation in determining non-built-up, built-up, and bare land areas.

Remote Sensing Indices	Built-Up Area	Bare Land
EBBI (Enhanced Built-Up and Bareness Index)	0.100–0.350	>0.350
IBI (Index-based Built-Up Index) [1]	0.018–0.308	>0.308
NDBI (Normalised Difference Built-Up Index) [6]	0.100–0.300	>0.300
UI (Urban Index)	>0	-
NDBaI (Normalised Difference Bareness Index) [4]	-	>−0.150

4.1. Mapping Built-Up and Bare Land

Table 3 shows the built-up areas as determined by each remote sensing transformation index. The results of the analysis showed that the total built-up area obtained from the EBBI transformation is 5,898.60 ha. This result is smaller than the amount of built-up area, 6,629.04 ha, that was determined from the IKONOS imagery. The built-up area shown by the EBBI is also smaller than that obtained from the IBI and NDBI transformations but is larger value obtained using the UI transformation.

Table 3. The built-up area from each type of index/remote sensing data transformation.

Remote Sensing Indices	Built-Up Area (ha)
EBBI	5,898.60
IBI	6,239.70
NDBI	5,934.33
UI	4,146.84
NDBaI	-
IKONOS	6,629.04

The areas of bare land in Serangan Island determined using the remote sensing indices are presented in Table 4. The area of bare land on Serangan Island as determined by the EBBI is 173.93 ha, which corresponds to 75.11% of the bare land area obtained from IKONOS imagery (231.39 ha). This percentage is higher than the bare land area determined using IBI and NDBI. However, the percentage of bare land indicated by the NDBaI is higher than that determined by EBBI. The overall spatial distribution of built-up and bare land areas obtained from the remote sensing indices and IKONOS data are shown in Figure 3.

Table 4. The bare land area in Serangan Island determined using each type of index/remote sensing data transformation.

Remote Sensing Indices	Bare Land Area (ha)
EBBI	173.79
IBI	105.21
NDBI	100.89
UI	-
NDBaI	197.82
IKONOS	231.39

The accuracy levels with respect to the percentage of built-up area for each type of transformation index from IKONOS data are shown in Table 5. The built-up area determined using the EBBI transformation was similar to that determined using the IKONOS data, which was assumed to represent the actual built-up area. A high level of accuracy was demonstrated when the IKONOS results were compared with the NDBI and UI transformations and negligible differences were observed between the IKONOS results and the IBI results. The percentage of similarity between the built-up area determined using the EBBI transformation compared to that from IKONOS was 69.65%; of this value, 25.49% of the IKONOS built-up area was transformed by EBBI into non-built-up area and 4.85% was transformed by EBBI into bare land area.

Table 6 presents the percentage accuracies of the results of each type of index transformation compared to the bare land area obtained from the IKONOS data. The percent accuracy of mapping bare land areas using the EBBI was also high (62.82%). This result is higher than the accuracy levels of the IBI and NDBI but lower than that of the NDBaI.

Figure 3. The spatial distribution of built-up areas and bare land is shown for each type of index/remote sensing data transformation: (a) EBBI, (b) IBI, (c) NDBI, (d) UI, (e) NDBal, and (f) IKONOS imagery.

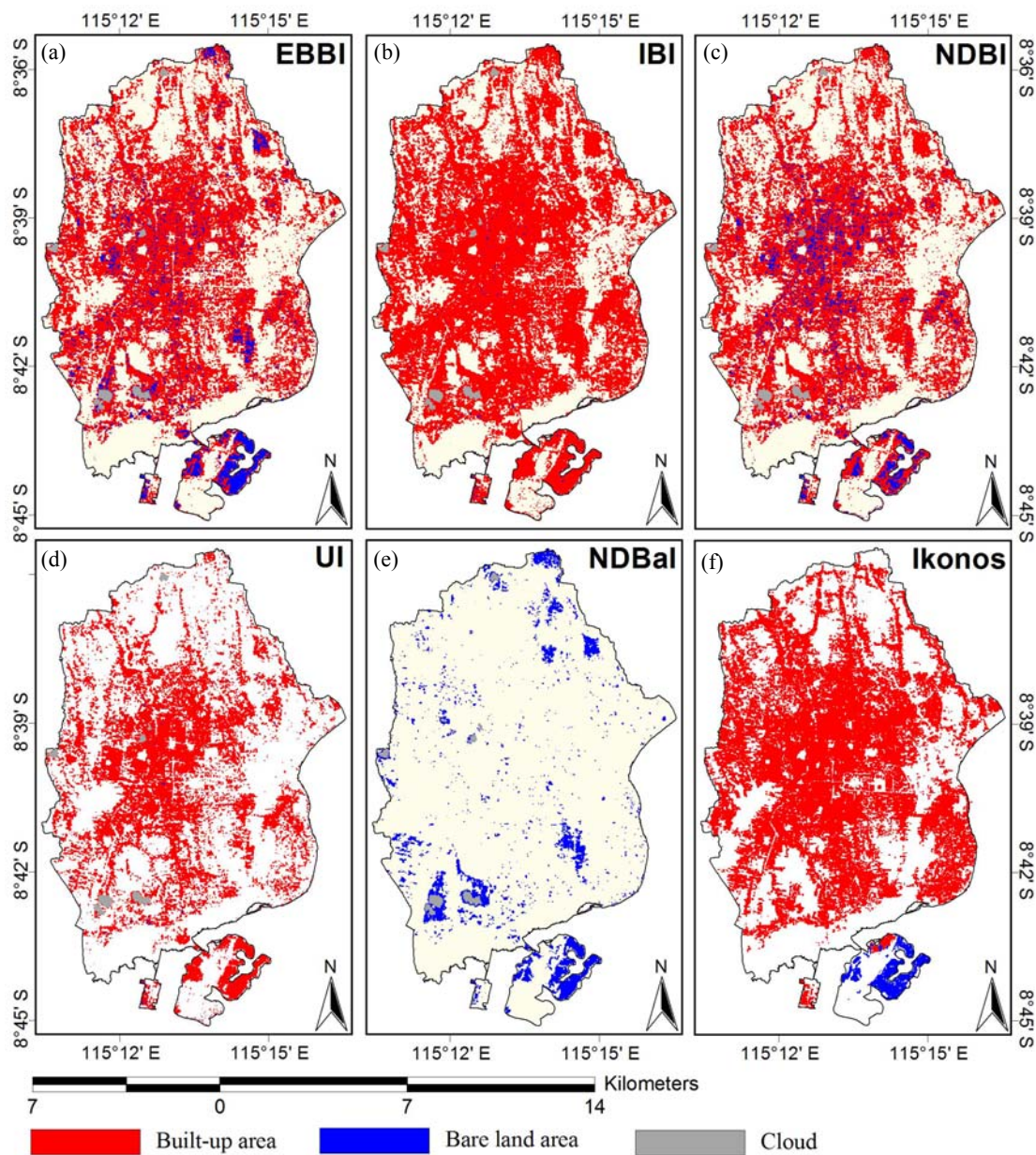


Table 5. The percent accuracy of the built-up area obtained from each type of index transformation.

Explanation	EBBI (%)	IBI (%)	NDBI (%)	UI (%)
Non-built-up area from indices vs. built-up area from IKONOS	25.49	21.71	25.05	47.11
Built-up area from indices vs. built-up Area from IKONOS	69.65	70.18	67.60	52.89
Bare land area from indices vs. built-up Area from IKONOS	4.85	8.11	7.34	—
Total built-up area from indices vs. Total built-up area from IKONOS	88.98	94.13	89.52	62.56

Table 6. The percent accuracies of the bare land area obtained from each type of index transformation.

Explanation	EBBI (%)	IBI (%)	NDBI (%)	NDBaI (%)
Non-bare land area from indices vs. bare land from IKONOS	13.73	12.10	13.15	31.74
Built-up area from indices vs. bare land area from IKONOS	23.45	49.59	50.72	–
Bare land area from indices vs. built-up area from IKONOS	62.82	38.31	36.13	68.26
Total bare land area from indices vs. total bare land area from IKONOS	75.11	45.47	43.60	85.49

When the average accuracy levels of the EBBI, NDBI, and IBI results were compared to those of the built-up and bare land area values obtained from IKONOS, the EBBI was found to exhibit the highest accuracy of all the indices. The EBBI exhibited an average accuracy level of 66.24%, which is higher than those of IBI and NDBI, which had average accuracy rates of 54.25% and 51.87%, respectively. The UI is an index that cannot detect bare land areas, while the NDBaI could not be used because it cannot map built-up areas.

The EBBI can be utilised directly as a highly accurate index for mapping built-up and bare land areas. Although the relative accuracy of the EBBI is lower than that of the IBI for mapping built-up areas and that of the NDBaI for mapping the distribution of bare land areas, the average accuracy level of EBBI represents a substantial improvement in the simultaneous mapping built-up and bare land areas.

4.2. Relationship between the Transformed Remote Sensing Indices and the Percentage of Built-Up Area

Figure 4 shows the relationship between the percentage of built-up area and the transformation indices (EBBI, IBI, NDBI, UI, NDBaI, and NDVI). The correlation coefficient and linear equation for each of the indices is indicated on the plot. A cross-plot of each index and the percentage of built-up area confirmed the close relationship between the EBBI results with the percentage of actual built-up areas. The relationship between the percentage of built-up areas and the EBBI results shows a high degree of correlation ($r = 0.70$). This correlation is higher than that of the five other remote sensing indices; the correlation values of the IBI, NDBI, UI, NDBaI, and NDVI are 0.61, 0.60, 0.59, 0.53, and 0.56, respectively.

The scatterplot indicates that the relationship between the EBBI results and the percentage of built-up area is generally higher than those of the other indices. In addition, statistical error analyses also demonstrated that EBBI generally produced lower values than the other indices, except with regard to MBE values, for which NDBaI produced higher values than EBBI. EBBI had an MBE value of 25.37%, while the MBE values of the IBI, NDBI, UI, NDBaI and NDVI were 60.03, 71.66, 57.84, –2.55, and 36.64%, respectively. Conversely, EBBI gave the lowest RMSE value (49.71%) relative to the other remote sensing transformation indices, while the IBI, NDBI, UI, NDBaI and NDVI gave RMSE values of 80.51, 89.01, 78.01, 50.84, and 112.06%, respectively. The summary of the statistical errors between the percentage of built-up area and the remote sensing transformation indices are shown in Figure 5.

Figure 4. Scatterplots of the built-up area percentage vs. the remote sensing transformation indices. (a) EBBI, (b) IBI, (c) NDBI, (d) UI, (e) NDBaI, and (f) Normalised Difference Vegetation Index (NDVI) .

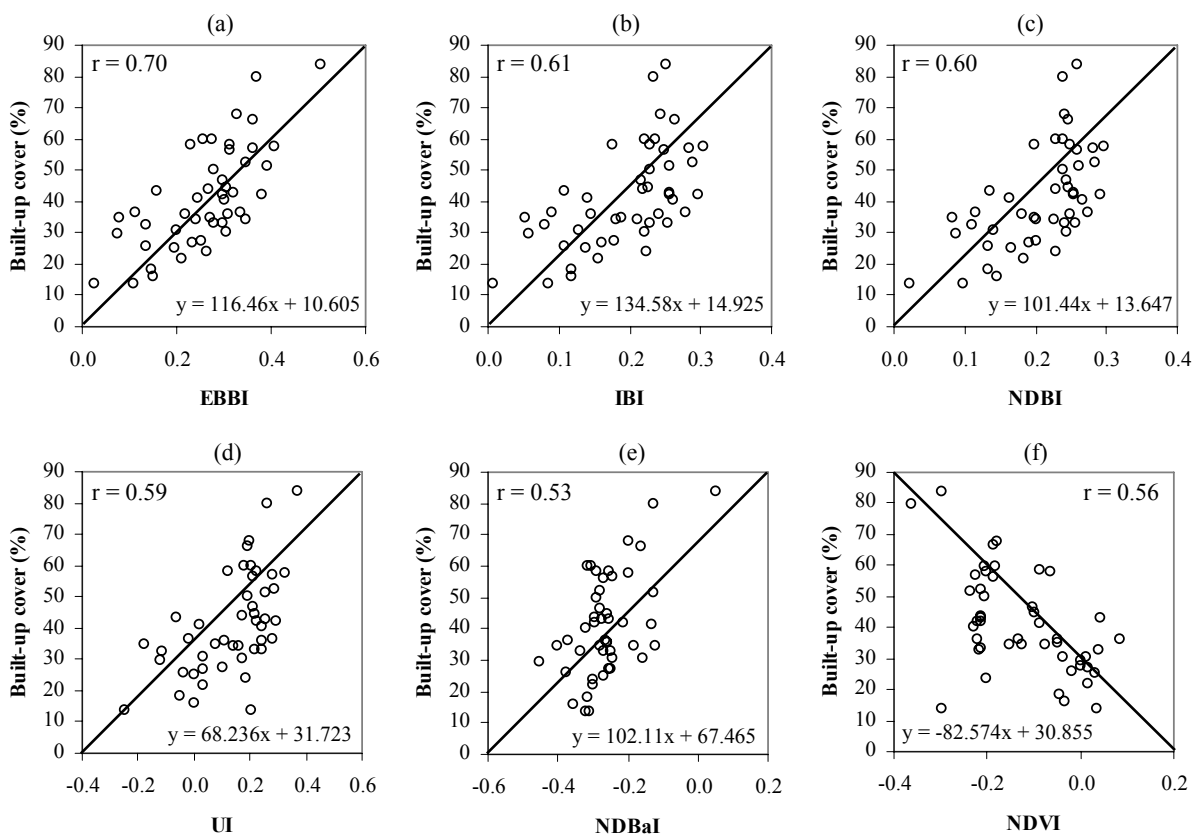
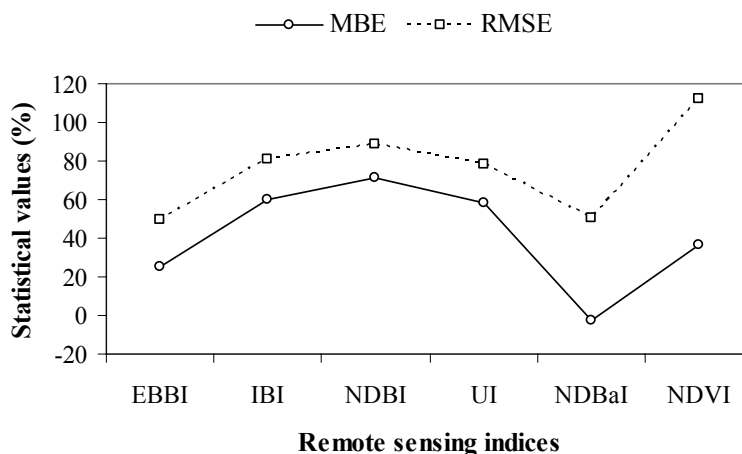


Figure 5. Mean bias error (MBE) and root mean square error (RMSE) statistical values between the percentage of built-up area and the remote sensing transformation indices.



5. Discussion

Urban remote sensing indices are generally used to distinguish built-up and bare land areas based on spectral values with a low level of accuracy because of the high degree of homogeneity in these land-use categories, especially in urban areas. However, utilisation of the EBBI, which is the first built-up and bare land index based on thermal infrared data, can increase the accuracy of mapping built-up and bare

land areas. The EBBI was also found to be very effective in distinguishing built-up and bare land areas, which is one of the major limitations of applying built-up area indices based on remotely sensed data. The use of three infrared channels (NIR, SWIR, and TIR) that reflect different contrasts in detecting built-up, bare land, and vegetation areas is responsible for the high accuracy level compared to other built-up area indices.

The application of TIR channels, which exhibit high emissivity in built-up areas, is one of the reasons that EBBI is a better index for distinguishing between classes of land use. The high emissivity in built-up areas is caused by the types of materials that are predominately found in these areas, such as roofing and building materials. In contrast, the emissivity of bare soil is determined by the level of soil moisture and by the mineral constituents of the soil [24]. Built-up areas exhibit higher heat conductivity than bare soil areas, resulting in the higher emissivity and albedo values of thermal infrared waves in built-up areas relative to bare soil areas.

The EBBI not only exhibits a better accuracy than other indices, but also was able to distinguish the amount of built-up areas with a higher correlation than other indices used in urban areas. The EBBI generally produced lower statistical errors regarding the measurement the built-up area percentage. The correlation levels between the percentage of built-up areas and the results of the other indices were all positive, with the exception of the results of NDVI. In addition, the MBE and RMSE values were generally lower than those determined by the other indices, with the exception of the MBE values, for which the value produced by NDBaI was better than that produced by EBBI. The utilisation of TIR channels and the improvement of the mathematical operations in the applied root function enhanced the statistical score regarding the percentage of built-up areas determined by the indices. TIR was also able to capture the temperature radiation released by buildings. Areas with relatively high building densities will emit larger amounts of temperature radiation. The root function applied in the EBBI contrasted identical objects based on different levels of reflectance values. The negative correlation exhibited by the NDVI was observed because this index is usually applied to rapidly map the distribution of vegetation. In NDVI, a smaller value indicates less vegetation, which results in a negative correlation with the amount of built-up areas. The relationships observed between the remote sensing indices and the amount of built-up area were similar to the results of previous studies, such as those of Widyasamratri [25] and Sukristiyanti *et al.* [11], who found the correlation coefficient between the UI-built-up area density in Semarang city to be 0.56 and 0.59, respectively.

The high degree of land homogeneity in built-up and bare land areas resulted in a low level of accuracy. Some regions in built-up areas were detected as non-built-up or bare land areas or were observed as noise in EBBI and NDBI images (Figure 3(a,c)). The spectral response of built-up areas showed a higher reflectance in the SWIR compared with the NIR wavelength range. However, in urban areas with heterogeneous landscapes, this factor is not always relevant. Drier vegetation or areas with mixed vegetation and buildings in a particular pixel can exhibit an even higher reflectance in the SWIR wavelength range than in the NIR range [26], thus leading to confusion with areas of built-up land. According to Yüksel *et al.* [27], accurate map processing in urban landscapes is further complicated by surface heterogeneity. Improving the spatial resolution may improve the accuracy of remote sensing in capturing small-scale objects over heterogeneous surfaces in urban areas [28].

Denpasar is a unique city because it contains a “holy area” in the centre of the town that is characterised by extensive vegetative cover near the built-up area. Additionally, canopy height

fluctuations in the centre of the town are substantial and may cover many different land use types. This creates a problem for subdividing urban areas into generalised classes of urban land uses and activities based on the spectral values of each individual pixel. Therefore, the accuracy of such techniques may decrease in regions with highly heterogeneous landscapes [29].

All the indices could not perfectly differentiate between built-up and bare land because both of these land types show similar spectral responses in all Landsat ETM+ bands. However, the EBBI was found to be superior to the other indices in distinguishing between built-up and bare land due to the use of TIR channels. Visual inspection of the extraction results showed that confusion mainly occurs between built-up areas and bare land areas. Mixed regions were detected by the EBBI as built-up in bare land areas in regions with a highly heterogeneous landscape, which exhibit high values in NIR and SWIR because of the drier vegetation. Generally, all of the findings of this study demonstrated that the EBBI could be utilised as an alternative and more accurate remote sensing index to distinguish built-up areas from other land use areas and determine the cover percentage of built-up areas.

Data from built-up areas are very important for determining correlations between land use and environmental conditions, such as air and water quality and water runoff. It is expected that in the future, the EBBI could be used in various applications associated with the utilisation of remote sensing data, specifically in the field of urban remote sensing. There are a number of potential applications for the EBBI, such as monitoring land use changes, following the development of cities, determining the condition of the urban environment, and calculating the urban population.

6. Conclusions

In this study, a new index for transforming remote sensing data was proposed and evaluated for mapping built-up and bare land areas. The index was able to map built-up and bare land areas with a single calculation and was referred to as the Enhanced Built-up and Bareness Index (EBBI). The EBBI is the first built-up and bare land index that uses the NIR, SWIR, and TIR channels simultaneously. The EBBI was applied in Denpasar, Indonesia, to distinguish between built-up and bare land in an urban area, and the results obtained by the EBBI were compared with those determined by other available remote sensing indices.

The use of the EBBI was found to improve the accuracy of mapping built-up and bare land areas. The EBBI was also effective at discriminating between built-up and bare land areas in an urban area. With regard to distinguishing between built-up and bare land areas with a single calculation, the EBBI showed an average accuracy level of 66.24%, which is higher than those of the IBI and NDBI (54.25% and 51.87%, respectively). The advantage of the EBBI is that it can be used not only to map built-up and bare land areas but is also capable of transforming the percentages of built-up land in urban area. Comparisons of the relationships between the percentages of built-up obtained from the EBBI and the five other remote sensing indices showed that the EBBI determines the built-up density percentage with higher accuracy (0.70) than the other indices.

Nevertheless, this proposed method has some limitations. Firstly, regions with highly heterogeneous landscapes are still problematic with respect to subdividing urban areas. Second, there are some limitations to using a single EBBI to distinguish between homogenous bare land and heterogeneous bare land mixed with drier vegetation or in urban areas, where higher levels of temperature radiation are emitted. Combining indices could improve the classification accuracy and,

thus, achieve better results. Finally, the EBBI was proposed to map built-up and bare land areas based on Landsat ETM+ bands. Thus, the generalisation of this index requires further experimentation using other satellite imagery with similar spectral bands.

References

1. Xu, H. A new index for delineating built-up land features in satellite imagery. *Int. J. Remote Sens.* **2008**, *29*, 4269–4276.
2. Melesse, A.M.; Weng, Q.; Thenkabail, P.S.; Senay, G.B. Remote sensing sensors and applications in environmental resources mapping and modelling. *Sensors* **2007**, *7*, 3209–3241.
3. As-Syakur, A.R.; Suarna, I.W.; Adnyana, I.W.S.; Rusna, I.W.; Laksmiwati, I.A.A.; Diara, I.W. Studi perubahan penggunaan lahan di DAS Badung. *Jurnal Bumi Lestari* **2010**, *10*, 200–207.
4. Zhao, H.M.; Chen, X.L. Use of Normalized Difference Bareness Index in Quickly Mapping Bare Areas from TM/ETM+. In *Proceedings of 2005 IEEE International Geoscience and Remote Sensing Symposium*, Seoul, Korea, 25–29 July 2005; Volume 3, pp. 1666–1668.
5. Weng, Q. Remote Sensing of Impervious Surfaces: An Overview. In *Remote Sensing of Impervious Surfaces*; Weng, Q., Ed.; CRC Press, Taylor & Francis Group: Boca Raton, FL, USA, 2008.
6. Chen, X-L.; Zhao, H-M.; Li, P-X.; Yin, Z-Y. Remote sensing image-based analysis of the relationship between urban heat island and land use/cover changes. *Remote Sens. Environ.* **2006**, *104*, 133–146.
7. Zha, Y.; Gao, J.; Ni, S. Use of normalized difference built-up index in automatically mapping urban areas from TM imagery. *Int. J. Remote Sens.* **2003**, *24*, 583–594.
8. Kawamura, M.; Jayamana, S.; Tsujiko, Y. Relation between social and environmental conditions in Colombo Sri Lanka and the urban index estimated by satellite remote sensing data. *Int. Arch. Photogramm. Remote Sens.* **1996**, *31 (Part B7)*, 321–326.
9. Rikimaru, A.; Miyatake, S. Development of Forest Canopy Density Mapping and Monitoring Model using Indices of Vegetation, Bare soil and Shadow. In *Proceeding of the 18th Asian Conference on Remote Sensing (ACRS) 1997*, Kuala Lumpur, Malaysia, 20–25 October 1997; p. 3.
10. He, C.; Shi, P.; Xie, D.; Zhao, Y. Improving the normalized difference built-up index to map urban built-up areas using a semiautomatic segmentation approach. *Remote Sens. Lett.* **2010**, *1*, 213–221.
11. Sukristiyanti, R.; Suharyadi; Jatmiko, R.H. Evaluasi Indeks Urban pada citra Landsat Multitemporal dalam ekstraksi kepadatan bangunan. *Jurnal Riset Geologi dan Pertambangan* **2007**, *17*, 1–10.
12. BPS. *Denpasar dalam Angka 2010*; Indonesian Central Bureau of Statistics: Denpasar, Indonesia, 2011.
13. Aldrian, E.; Susanto, D.R. Identification of three dominant rainfall regions within Indonesia and their relationship to sea surface temperature. *Int. J. Climatol.* **2003**, *23*, 1435–1452.
14. As-Syakur, A.R.; Tanaka, T.; Prasetia, R.; Swardika, I.K.; Kasa, I.W. Comparison of TRMM multisatellite precipitation analysis (TMPA) products and daily-monthly gauge data over Bali. *Int. J. Remote Sens.* **2011**, *32*, 8969–8982.

15. As-Syakur, A.R.; Osawa, T.; Adnyana, I.W.S. Medium spatial resolution satellite imagery to estimate gross primary production in an urban area. *Remote Sens.* **2010**, *2*, 1496–1507.
16. Herold, M.; Roberts, D.A.; Gardner, M.E.; Dennison, P.E. Spectrometry for urban area remote sensing—Development and analysis of a spectral library from 350 to 2400 nm. *Remote Sens. Environ.* **2004**, *91*, 304–319.
17. Herold, M.; Gardner, M.E.; Roberts, D.A. Spectral resolution requirements for mapping urban areas. *IEEE Trans. Geosci. Remote Sens.* **2003**, *41*, 1907–1919.
18. Lu, D.; Weng, Q. Use of impervious surface in urban land-use classification. *Remote Sens. Environ.* **2006**, *102*, 146–160.
19. Gers, C.J. *Relating Remotely Sensed Multi-Temporal Landsat 7 ETM+ Imagery to Sugarcane Characteristics*; South African Sugar Association Experiment Station: Mount Edgecombe, South Africa, 2003.
20. Tucker, C.J. Red and photographic infrared linear combinations for monitoring vegetation. *Remote Sens. Environ.* **1979**, *8*, 127–150.
21. Matthias, B.; Martin, H. Mapping imperviousness using NDVI and linear spectral unmixing of ASTER data in the Cologne-Bonn region (Germany). *Proc. SPIE* **2003**, *5239*, 274–284.
22. Willmott, C.J. Some comments on the evaluation of model performance. *Bull. Amer. Meteorol. Soc.* **1982**, *63*, 1309–1313.
23. Willmott, C.J.; Ackleson, S.G.; Davis, R.E.; Feddema, J.J.; Klink, K.M.; Legates, D.R.; O'Donnell, J.; Rowe, C.M. Statistics for the evaluation and comparison of models. *J. Geophys. Res.* **1985**, *90*, 8995–9005.
24. Lesaignoux, A.; Fabre, S.; Briottet, X.; Olioso, A. Influence of Surface Soil Moisture on Spectral Reflectance of Bare Soil in the 0.4–15 μm Domain. In *Proceedings of the 6th EARSeL SIG IS Workshop*, Tel-Aviv, Israel, 16–19 March 2009; p. 6.
25. Widyasamratri, H. Utilization of Urban Index and Vegetation Index Transformation on ASTER Image Satellite for Analysis Urban Environment Condition (Case: Semarang Municipality). In *Proceedings of 10th N-AERUS Conference 2009*, Rotterdam, The Netherland, 1–3 October 2009.
26. Gao, B.C. NDWI—A normalized difference water index for remote sensing of vegetation liquid water from space. *Remote Sens. Environ.* **1996**, *58*, 257–266.
27. Yüksel, A.; Akay, A.E.; Gundogan, R. Using ASTER imagery in land use/cover classification of eastern Mediterranean landscapes according to CORINE land cover project. *Sensors* **2008**, *8*, 1237–1251.
28. Tran, T.-B.; Puissant, A.; Badariotti, D.; Weber, C. Optimizing spatial resolution of imagery for urban form detection—The cases of France and Vietnam. *Remote Sens.* **2011**, *3*, 2128–2147.
29. Soegaard, H.; Møller-Jensen, L. Towards a spatial CO₂ budget of a metropolitan region based on textural image classification and flux measurements. *Remote Sens. Environ.* **2003**, *87*, 283–294.